Proc. Indian Acad. Sci. (Chem. Sci.), Vol. 111, No. 3, June 1999, pp. 397–411

Salicylaldoxime: An old ligand with new faces

PHALGUNI CHAUDHURI
Max-Planck-Institut für Strahlenchemie, D-45470 Mülheim an der Ruhr, Germany
e-mail: chaudh@mpi-muelheim.mpg.de

Abstract. The paper is concerned with the interactions of salicylaldoxime with trivalent transition metal ions to yield di-, tri-, tetra- and hexanuclear complexes together with their low-lying electronic structures. Tri- and tetranuclear complexes are found to exhibit spin frustration. The importance of isostructural series of compounds with varying d^n electron configurations is indicated. Relevance of some of these compounds as models for metalloproteins is also shown.

Keywords. Salicylaldoxime; transition metal ions; polynuclear complexes; magnetochemistry; spin frustration.

1. Introduction

Salicylaldoxime was used first as a ligand for complexation of metal ions by F Ephraim [1] as early as in 1930. X-ray structural reports [2] on the square-planar complexes of the divalent metals Ni(II), Pd(II) and Pt(II) were published shortly after that in 1935. Surprisingly there are only very few structural reports [3–14] on the salicylaldoximato-complexes. Moreover, reports on the ligating properties of salicylaldoxime towards the trivalent transition metal ions [10,15] are nearly missing. Here we provide a brief account of our findings on the ligating properties of salicylaldoxime.

Exchange-coupled clusters of transition metal ions are relevant to many different scientific areas, ranging from chemistry to solid-state physics and to biology, because of their potential impact on material science, catalysis and metallo-biochemistry. The ubiquitous participation of metal sites involving more than one metal centre in metalloproteins has elicited the interest of bioinorganic chemists in such interactions. It is worth mentioning in this connection that investigations of a series of isostructural polynuclear complexes with varying d^n-electrons are more informative in comparison to those of singly-isolated exchange-coupled clusters. The presence of different competing interactions owing to the topologies in polynuclear complexes may lead to ground and other low-lying states that cannot be expected by simple combination of the local spins according to the nature of the interactions present between the spin carriers. We will demonstrate in this report several examples of such ground-state variability due to spin frustration.

2. Ligands and their abbreviations

The structures of the ligands and the abbreviations used for them are as shown in chart 1.

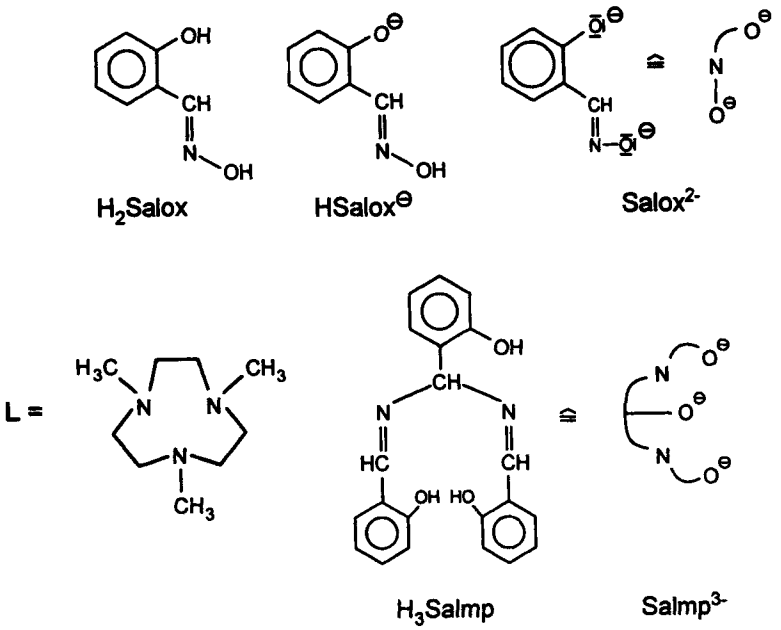

Chart 1. Structure of the ligands used.

3. Results and discussion

3.1 *Dinuclear complexes*

Our continuing interest in metal-oximates as building blocks for synthesizing homo- and heteropolynuclear complexes led us to use *tris*(salicylaldoximato)metallate(III) as ligands for a ML fragment, where M represents a trivalent transition metal ion and L the tridentate cyclic amine 1,4,7-trimethyl-1,4,7-triazacyclononane, which coordinates facially in octahedral complexes. Our synthetic strategy is depicted in scheme 1.

Obviously M_A and M_B in the scheme could be either same or dissimilar yielding homo- or hetero-dinuclear complexes. Thus a series of dinuclear complexes (table 1) containing homo- or hetero-metal centres has been synthesized and characterized by X-ray crystallography, variable-temperature (2–290 K) susceptibility measurements, different spectroscopic (EPR, Mössbauer, UV-VIS) and electrochemical methods. The compounds exhibit notably not only metal-centred but also ligand-centred oxidations (i.e. formation of phenoxyl radical), as is evident from the electronic, EPR and Mössbauer spectra of the oxidized species generated by the controlled potential electrolysis. The exchange coupling constants are listed in table 1.

These dinuclear complexes [16] are well suited for studying interactions of phenoxyl radicals with transition metal ions. Table 1 is not complete and we expect to add more dinuclear complexes to it in the near future.

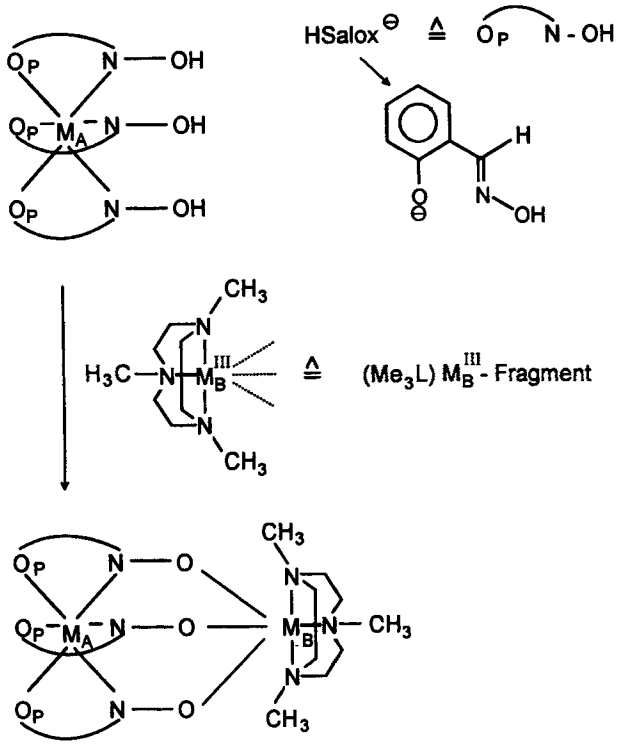

Scheme 1.

Table 1. Exchange coupling constants for the dinuclear complexes containing the M(Salox)$_3$-unit ($H = -2JS_1 \cdot S_2$)

Complex	J (cm^{-1})	Complex	J (cm^{-1})
$LFe^{III}(Salox)_3Fe^{III}$	−11·9	$LMn^{IV}(Salox)_3Mn^{III}$	−5·6
$LMn^{III}(Salox)_3Mn^{III}$	+6·5	$LMn^{IV}(Salox)_3Fe^{III}$	+14·8
$LMn^{III}(Salox)_3Fe^{III}$	−4·9	$LFe^{III}(Salox)_3Ga^{III}$	μ_{eff} = 5·53–5.90 μ_B (4–293 K)

As a representative one, the X-ray structure and a cyclic voltammogram of $LFe^{III}(Salox)_3Fe^{III}$ are shown in figures 1 and 2. Both iron centres are in distorted octahedral geometry and high-spin with d^5 electron configuration, as is evident from the metrical parameters for the Fe–O and the Fe–N bond lengths (figure 1). Effective magnetic moment μ_{eff} decreases monotonically from 6·86 μ_B at 290 K reaching a value of 0·15 μ_B at 2 K, indicating a diamagnetic ground state. The antiferromagnetic exchange coupling constant was evaluated to be $J = -11{\cdot}9$ cm^{-1} by simulation of the experimental magnetic data using a least-squares fitting computer program with the spin Hamiltonian $H = -2JS_1 \cdot S_2$ (with $S_1 = S_2 = 5/2$).

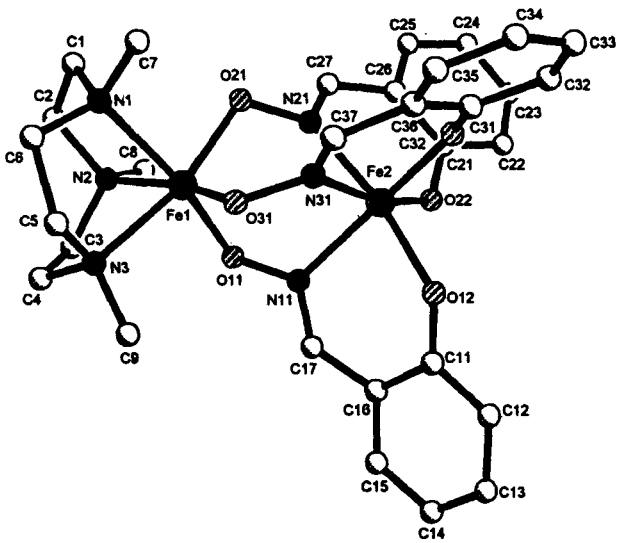

Figure 1. Structure of [LFe(Salox)$_3$Fe]: Fe(1)...Fe(2) 3·57 Å, Fe(1)–N 2·23 Å, Fe(1)–O 1·95 Å, Fe(2)–N 2·16 Å, Fe(2)–O 1·95 Å; twist angles Fe(1)N_3O_3 52·5°, Fe(2)N_3O_3 47°.

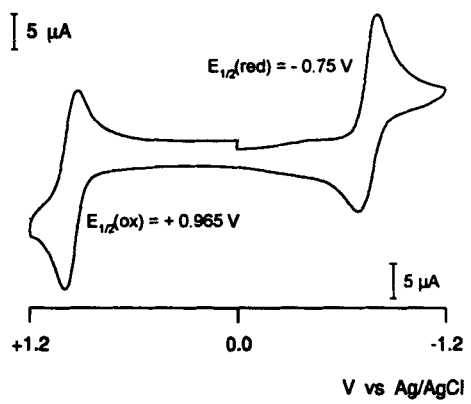

Figure 2. CV of [LFe(Salox)$_3$Fe] in CH_3CN at 22°C; GC electrode, scan rate 200 mV s^{-1}. $E_{1/2}$(ox) = 0·965 V, $E_{1/2}$(red) = –0·75 V, vs Ag/AgCl.

3.2 *Trinuclear complexes*

The route used for the synthesis of the trinuclear M(III) complexes is a general one and has been used to prepare the isostructural compounds containing the unprecedented asymmetric triangular M(III) complexes with the $[M^{III}_3(\mu_3\text{-O})(\mu_2\text{-OPh})]^{6+}$ structural unit[17,18]. We have found that the core $[M^{III}_3(\mu_3\text{-O})(\mu_2\text{-OPh})]^{6+}$ is ubiquitous and can be

obtained for Ti(III), V(III), Cr(III), Mn(III), Fe(III) and Co(III) with the general composition

$$[Et_3NH][M^{III}{}_3(\mu_3\text{-}O)(Salox)_2(HSalox)(Salmp)].$$

Except for the corresponding Ti(III) complex, all other complexes are characterized crystallographically.

The iron(III) and vanadium(III) complexes only are described here to demonstrate the phenomenon of *spin frustration*, and to present the iron-complex containing an isosceles triangular arrangement of the ferric ions as a potential structural model for the iron-binding site 3 in ferreascidin [19], a glycoprotein isolable from the blood cells of the stolidobranch ascidian (*Pyura stolonifera*), as the iron-complex shares many, but not all, of the characteristics of site 3.

The asymmetric triangular M^{III}-compounds have been obtained by an unusual M^{II}-promoted activation [20] of salicylaldoxime. The *in situ* formation of the ligand H_3Salmp, [2-(*bis*(salicylideneamino)-methyl)phenol], from the starting salicylaldoxime is believed to occur by the reaction pathway involving reductive deoximation shown in scheme 2.

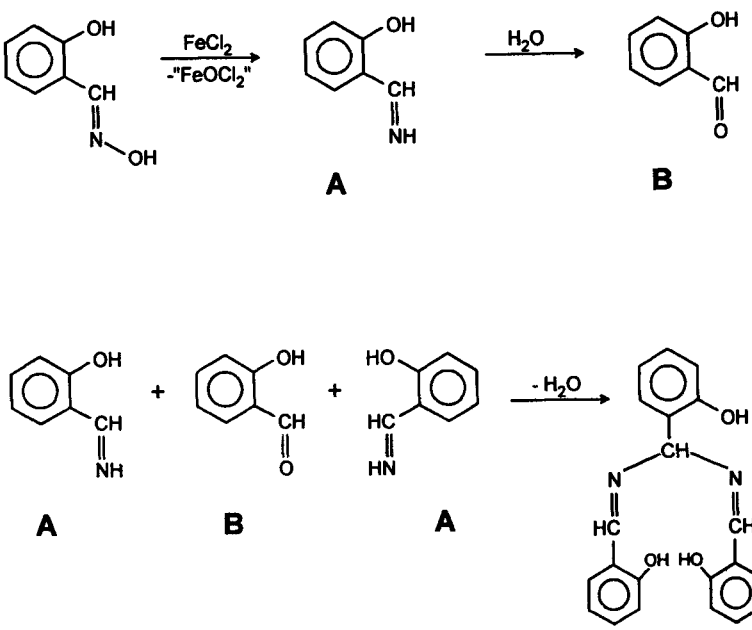

Scheme 2

The molecular structure containing the trinuclear core $[Fe_3(\mu_3\text{-}O)(\mu_2\text{-}OPh)]^{6+}$, shown in figure 3, and highlighting the coordination spheres of the three iron atoms, is an archetype of the trinuclear complexes described here. The iron ions Fe(1) and Fe(2) are in distorted octahedral environments, having FeN_2O_4 coordination spheres, and Fe(3) is in a trigonal bipyramidal $FeNO_4$ environment. The uninegative charge of the anion in the ferric complex leads us to conclude that the oxygen O(32) of the hydroxy group in the salicylaldoxime bonded only to Fe(3) is protonated. A moderately strong hydrogen bond

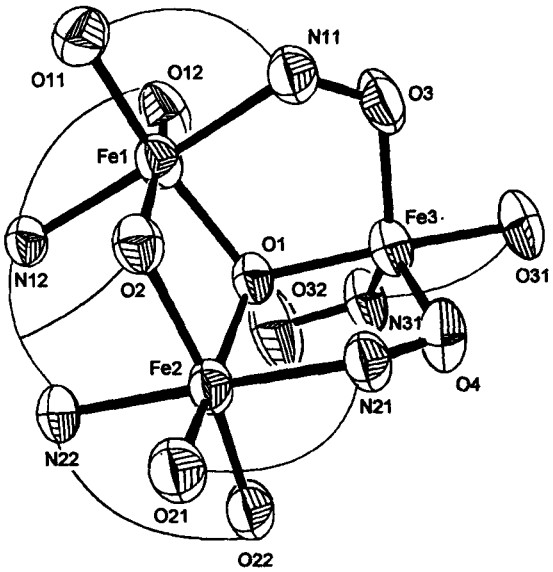

Figure 3. Molecular structure of the trinuclear ferric complex containing the core $[Fe_3(\mu_3\text{-}O)(\mu_2\text{-}OPh)]$.

may be envisaged between O(32) and O(1) with the distance O(32)...O(1) of 2·68 Å. The Fe–N and Fe–O bond distances are consistent with a d^5 high-spin electron configuration of the Fe^{III} centres with azomethine nitrogen and phenolate oxygen-donor ligands.

The Fe(2)...Fe(1) distance, 3·065(1) Å, is noticeably shorter than the Fe(2)...Fe(3) and Fe(1)...Fe(3) distances, 3·348(1) and 3·342(1) Å, respectively. The disposition of the μ_3-oxide O(1) is not symmetrical, the differences being significant, Fe(1)–O(1) 1·982(5) Å, Fe(2)–O(1) 1·968(5) Å and Fe(3)–O(1) 1·917(5) Å.

The exchange coupling model[17] used to analyze the variable-temperature magnetic susceptibility data contains two J's, $J_{23} = J_{13} = J$ describing the interaction of Fe(3) with Fe(2) and Fe(1), $J_{12} = J'$ the interaction between the Fe(2) and Fe(1) ions, as the trinuclear iron(III) framework forms an isosceles triangle. The magnetic measurements reveal an $S_t = 5/2$ ground state with antiparallel exchange interactions $J = -34{\cdot}3\ cm^{-1}$, $J' = -4{\cdot}7\ cm^{-1}$ and $D = -0{\cdot}90\ cm^{-1}$. The EPR results are consistent with a ground state of $S = 5/2$ together with a negative $D_{5/2}$ value. The Mössbauer isomer shifts together with the quadrupole splittings also provide evidence for the high-spin state of the ferric sites:

$$\delta = 0{\cdot}45\ mm\ s^{-1},\ \Delta E_Q = -1{\cdot}10\ mm\ s^{-1} \text{ for Fe(3)}$$

$$\delta = 0{\cdot}49\ mm\ s^{-1},\ \Delta E_Q = -0{\cdot}63\ mm\ s^{-1} \text{ for Fe(1)/Fe(2).}$$

Magnetic Mössbauer spectra (1·5 K; 3.5 and 7 T) lead to the conclusion that the internal magnetic fields possibly lie in the plane of the three ferric ions.

A *linear* trinuclear Fe^{III} cluster as the structure for the metal-ion binding site 3 of ferreascidin has been proposed[19] on the basis of its paramagnetic ground state with $S = 5/2$. μ-oxo, μ-hydroxo and μ-phenoxo groups have been considered as candidates for

the bridging ligands, although no unequivocal identification of the bridging ligands present at site 3 could be made. The triangular μ_3-oxo bridged Fe^{III} structural motif present in the "basic Fe(III)-carboxylates" has been eliminated, because the lowest spin state of the known trinuclear carboxylates is $S = 1/2$, which is inconsistent with the $S = 5/2$ ground state of the protein. Keeping these points in mind, the $[Fe^{III}_3(\mu_3\text{-O})(\mu_2\text{-OPh})]^{6+}$ core, stabilized by the ligands salicylaldoxime and H_3Salmp, is a potential candidate for the site 3 of ferreascidin.

The trinuclear V(III) complex [18] exhibits identical isosceles triangular structure with very similar metrical parameters; hence we refrain from discussing the same in detail. But a short account of its magnetic properties is essential for the forthcoming discussion on the presence of spin frustration effects arising in certain topological arrangements of metal ions possessing competing pairwise exchange interactions of comparable magnitude. We employ the term "spin frustration" for the general situation [21] where competing exchange interactions of comparable magnitude lead to the prevention (frustration) of preferred spin alignments, and not in the sense of "orbital degeneracy" [22].

The ground state with $|S_t = 1, S^* = 0\rangle$, which lies 45·7 and 61·8 cm^{-1} below the first $|S_t = 2, S^* = 1\rangle$ and second $|S_t = 1, S^* = 1\rangle$ excited states respectively, is revealed from the simulation of the experimental magnetic data by using a computer program with a full-matrix diagonalization approach using the $H = -2JS_i \cdot S_j$ convention. The $S_t = 1$ ground state is also confirmed by the field-dependent magnetization study at 2 K in the 0·5–7·0 T magnetic field range (figure 4); the solid line in figure 4 is the calculated curve with the following parameter set, which has also been used for the simulation of the susceptibility data.

$J_{13} = J_{23} = 4{\cdot}0\ cm^{-1}$; $J_{12} = -26{\cdot}9\ cm^{-1}$;
$D_1 = D_2 = 2{\cdot}9\ cm^{-1}$ (fixed); $D_3 = 1{\cdot}5\ cm^{-1}$ (fixed);
$g_1 = g_2 = 1{\cdot}87$ (fixed); $g_3 = 1{\cdot}97$ (fixed); No TIP.

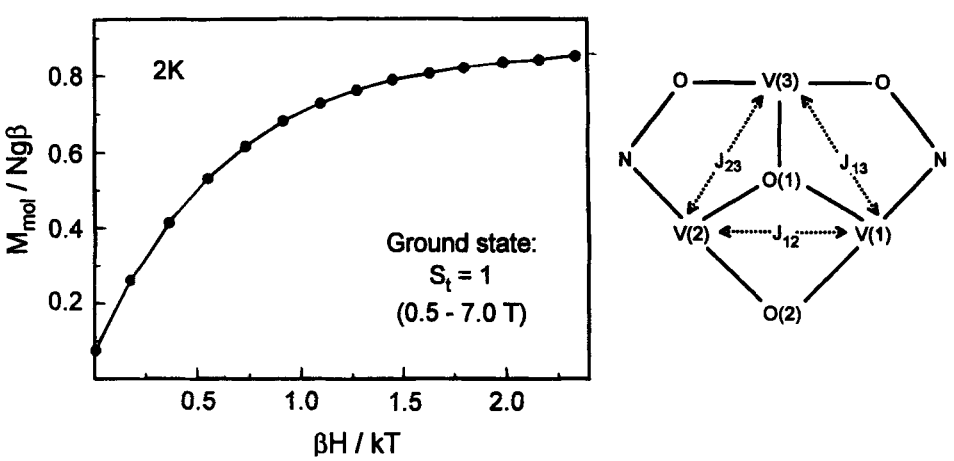

Figure 4. Field-dependent magnetizations at 2 K for the trinuclear V(III) complex. The solid line is the calculated curve.

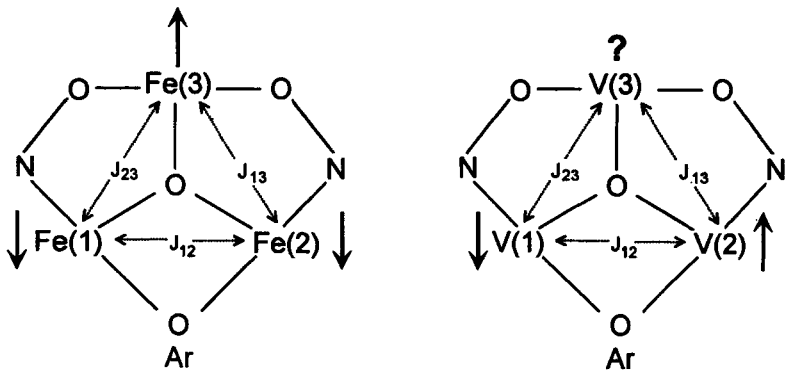

Figure 5. Spin frustration in Fe^{III}_3 and V^{III}_3-complexes.

Spin frustration results naturally from the triangulated topological arrangement of metal ions. If all of the pairwise interactions in the Fe^{III}_3-triangle are antiferromagnetic, as is the case here, the origin of this frustration is easily understood. The spins on each Fe(3)/Fe(1) and Fe(3)/Fe(2) couples are paired, because these antiparallel interactions ($J = -34{\cdot}3\ cm^{-1}$) dominate over the interaction between the Fe(1) and Fe(2) ions ($J' = -4{\cdot}7\ cm^{-1}$). This frustrates the spins on the Fe(1) and Fe(2) ions, as the intrinsic nature of this interaction (J') is antiferromagnetic. The unpaired electrons on Fe(1) and Fe(2) want to pair, but they are frustrated and hence they cannot. The situation is depicted not only for Fe^{III}_3 but also for the V^{III}_3 complex (figure 5). Interestingly, the J_{12} interaction dominates over J_{13}/J_{23} interaction, thus making the V(3) ion frustrated.

3.3 *Tetranuclear complexes with the "butterfly" core* $[(M_A)_2(\mu_3\text{-}O)_2(M_B)_2]^{8+}$

The synthesis of the tetranuclear complexes, together with that of the dinuclear complexes, is outlined in scheme 3.

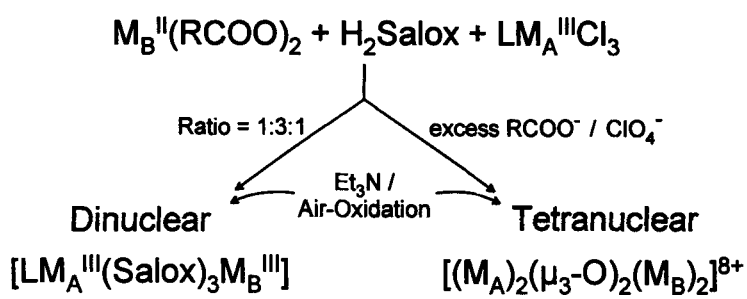

Scheme 3

The concern of this section is the compounds with the general formula

$[L_2(M_A)_2(\mu_3\text{-}O)_2(M_B)_2(Salox)_2(\mu_2\text{-}RCOO)_3]^+$
where M_A = Fe(III); M_B = Fe(III),
or M_A = Mn(III); M_B = Mn(III),
or M_A = Fe(III); M_B = Mn(III),

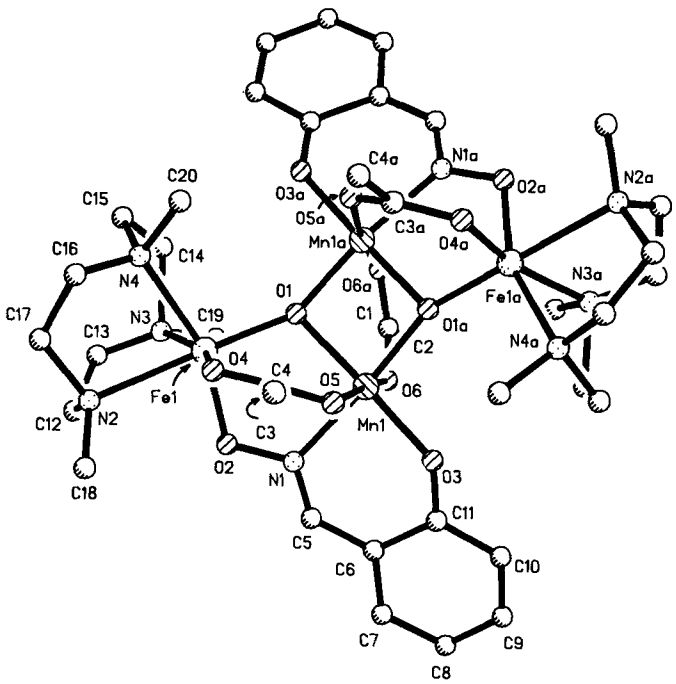

Figure 6. Molecular structure of the monocation $[L_2Fe_3(\mu_3\text{-}O)_2(Salox)_2\text{-}(\mu_2\text{-}CH_3COO)_3Mn_2]^+$.

in which the high-spin M(III) ions are disposed in a butterfly arrangement. The corresponding $[Cr^{III}_2(\mu_3\text{-}O)_2Fe^{III}_2]^{8+}$ and $[Cr^{III}_2(\mu_3\text{-}O)_2Mn^{III}_2]^{8+}$ cores are also known,[23,24] but will not be discussed here.

Most of the compounds discussed below are characterized crystallographically; the structure of the $[Fe_2Mn_2(\mu_3\text{-}O)_2]$-core only is described to demonstrate the atom-connectivities in this class of tetranuclear complexes. The structure of the cation is presented in figure 6. The metal geometry may be described as a "butterfly" based on two edge-sharing $FeMn_2O$ triangular units with the oxygen atoms O(1) below and O(1a) above the corresponding $FeMn_2$ triangles. The dispositions of μ_3-oxides are almost symmetrical. In addition to the two μ_3-oxo groups, there are three bridging acetate groups, one each between Fe(1)Mn(1), Fe(1a)Mn(1a) and Mn(1)Mn(1a) pairs. Additionally, two –[N–O] groups of the deprotonated oximes are coordinated through oxygen to the iron and through the nitrogen to the manganese of the pairs Fe(1)Mn(1) and Fe(1a)Mn(1a). The manganese and iron atoms that are carboxylate bridged are apparently "pulled" closer to one another, Fe(1)...Mn(1) 3·19 Å, than those that are without carboxylate bridging, Fe(1)...Mn(1a) 3·72 Å. The Mn(1) and Mn(1a) atoms, constituting the "body" metal atoms, are also carboxylate-bridged and the distance between them is noticeably short, 2·81 Å. The M–N and M–O bond distances are consistent with those of high-spin Fe(III) and Mn(III) coordination complexes. The distance between the "wing-tip" irons is long, 6·05 Å.

The temperature dependence of the magnetic susceptibility unambiguously reveals a non-degenerate $S_t = 0$ ground state, well isolated in energy, for the $[Fe_4(\mu_3\text{-}O)_2]^{8+}$ core, not only for the *acetate*, but also for the *benzilate* and *triphenylacetate* as the bridging carboxylate groups. Interestingly, for the $[Mn_4(\mu_3\text{-}O)_2]^{8+}$ core, the ground state is

established to be $S_t = 3$ from the magnetic susceptibility as well as from the field-dependent (0·5–7·0 T) magnetization measurements at 2 K for all the bridging carboxylates used, viz. *acetate*, *chloroacetate*, *triphenylacetate*, *benzoate* and *benzilate* ligands. As for example, the following parameters are evaluated for the tetramanganese compound with the bridging *benzilate* ion.

$$J_{\text{body-body}} = J_{bb} = J_{MnMn} = -10{\cdot}2 \text{ cm}^{-1}; J_{\text{wing-body}} = J_{wb} = J_{FeMn} = +0{\cdot}48 \text{ cm}^{-1};$$
$$g = 2{\cdot}09; D = 9{\cdot}0 \text{ cm}^{-1}.$$

On the contrary, the triplet ($S_t = 1$) ground state $|1,4,5\rangle$ for the acetate-bridged $[Fe_2Mn_2(\mu_3\text{-}O)_2(CH_3COO)_3]^{5+}$ core has components S_{Mn} and S_{Fe} values of 4 and 5, respectively, and the overall favoured spin alignment is shown with the exchange coupling constants in chart 2.

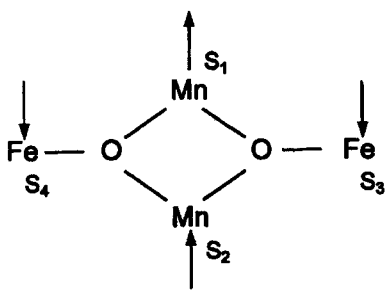

$J_{FeMn} = -25{\cdot}7 \text{ cm}^{-1}$
$J_{MnMn} = -35{\cdot}8 \text{ cm}^{-1}$
$g = 2{\cdot}06$

Chart 2. Spin frustration.

The first excited spin-quintet state $|2,3,5\rangle$ is placed 22 cm^{-1} above the ground state $|1,4,5\rangle$. The energy difference between the lowest two states has been found to be $\Delta E = 26 \pm 6 \text{ cm}^{-1}$ from the EPR measurements (5–50 K), thus confirming the results of the susceptibility data. Although the intrinsic interaction between the "body" manganese ions of the butterfly is antiparallel in nature, there is frustration in the spin alignment associated with the two manganese ions, causing the alignment to be parallel.

The carboxylic bridging ligands have been varied for the Fe_2Mn_2-core, viz. *acetic, propionic, chloroacetic, benzilic, benzoic* and *triphenylacetic* acids. It is evident from table 2, that the ground states evaluated by the field-dependent (0·5–7·0 T) magnetization measurements at 2 K are *different for different carboxylic bridging ligands*, implying that the "R" groups of the carboxylic acids might not be that innocent, as is commonly taken for granted. It is noteworthy in this connection that the ratio J_{bb}/J_{wb}, and not the absolute values of J_{bb} and J_{wb}, is determinant for the ground state. The ratio varies from 1·4 to 2·1 for the aforementioned carboxylates, as is illustrated in table 2. As a representative plot, the field-dependent magnetization measurements for the triphenylacetate bridged $[Fe_2Mn_2(\mu_3\text{-}O)_2(Ph_3CCOO)_3]^{5+}$ unit are shown in figure 7.

Figure 8 is a spin-correlation diagram for the Fe_2Mn_2-butterfly arrangement in which the energy of a state is plotted as a function of the ratio J_{bb}/J_{wb}. The correlation diagram clearly demonstrates the ground state variation as a function of the ratio J_{bb}/J_{wb}, which is also constituent with the experimental findings for the different carboxylate bridging ligands with the heterometallic Fe_2Mn_2-core.

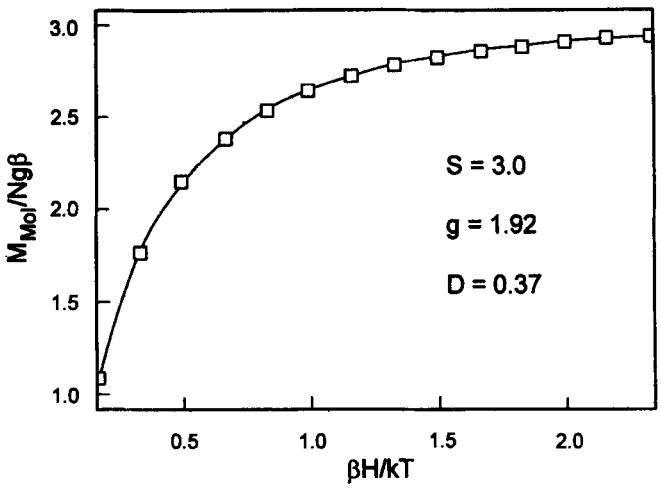

Figure 7. Field dependent magnetizations at 2 K for $[L_2Fe_2(\mu_3\text{-}O)_2(Salox)_2\text{-}(\mu_2Ph_3CCOO)_3Mn_2]ClO_4$.

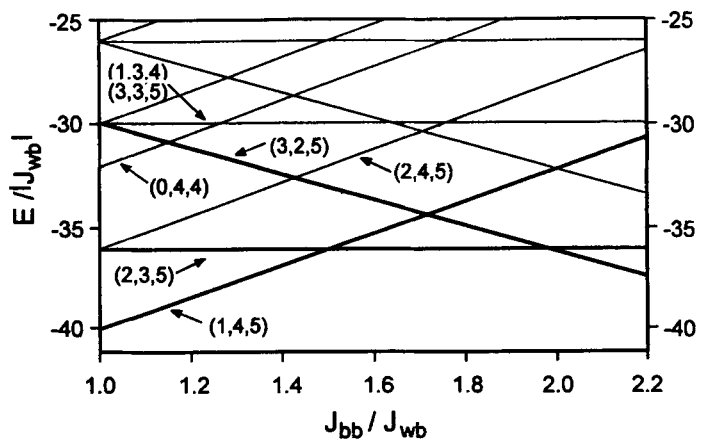

Figure 8. A spin-correlation diagram for the Fe_2Mn_2-complex.

Table 2. Ground state evaluation by magnetization measurements at 2 K for the $[Fe^{III}{}_2(\mu_3\text{-}O)_2Mn^{III}{}_2]^{8+}$ core containing different carboxylates

Carboxylic acid	Ground state magnetization (0·5–7·0 T) at 2 K	$J_{bb}/J_{wb} = J_{MnMn}/J_{FeMn}$
Acetic acid	$S_t = 1$	1·39
Propionic acid	$S_t = 1$	1·34
Chloroacetic acid	$S_t = 2$	1·68
Benzilic acid	$S_t = 2$	1·63
Benzoic acid	$S_t = 3$	2·03
Triphenyl acetic acid	$S_t = 3$	2·09

To conclude this section, we want to mention that the identity of the wing-tip ions as the ferric ions, and not Mn(III), has been checked by comparing the Mössbauer parameters of the Fe_2Mn_2-complexes with those of the Fe_4-complexes. The isomer shifts (δ_{Fe}) at 80 K for the Fe_2Mn_2-complexes lie in the range 0·45–0·47 mm s^{-1}, showing clearly that the "wing-tip" positions are occupied by the high-spin Fe(III) ions.

3.4 *Hexanuclear complexes with the $[M^{III}{}_6(\mu_3\text{-}O)_2]$ core (M = V, Cr, Mn, Fe)*

We have discovered that the hexanuclear M^{III} complexes containing the structural core $[M^{III}{}_6(\mu_3\text{-}O)_2]$ are not very unusual species and can be obtained for V^{III}, Cr^{III}, Mn^{III} and Fe^{III} through a general synthetic route. The hexanuclear compounds with the general composition

$$[M^{III}{}_6(\mu_3\text{-}O)_2(Salox)_6(\mu_2\text{-}OOCR)_2(OH_2)_2(RCN)_2],$$

where Salox represents the dianion of salycylaldoxime, $RCOO^-$ carbooxylate anions such as triphenylacetate, pivalate, benzilate, benzoate or propionate, and RCN a nitrile solvent like acetonitrile, propionitrile or butyronitrile, have been structurally characterized[25] and found to be isotypic. A view of the first coordination spheres of Cr^{III}-ions is shown in figure 9, as an archetype of the hexanuclear complexes.

The six chromium atoms in the hexanuclear structure are distributed in two μ_3-oxo-centred trinuclear arrays $[Cr_3(\mu_3\text{-}O)]$, which are bridged through the oxygen atoms O(3) and O(3a) of the oxime moiety. The chromium atoms Cr(2) and Cr(2a), belonging to the two separate $Cr_3(\mu_3\text{-}O)$ units, are separated by a distance of 3·275(1) Å. The chromium atoms Cr(1), Cr(2) and Cr(3) form an isosceles triangle with the following separations: Cr(1)...Cr(2) 3·148(1), Cr(1)...Cr(3) 3·263(1) and Cr(2)...Cr(3) 3·252(1) Å. The chromium atoms Cr(2) and Cr(3) are in distorted octahedral environments having

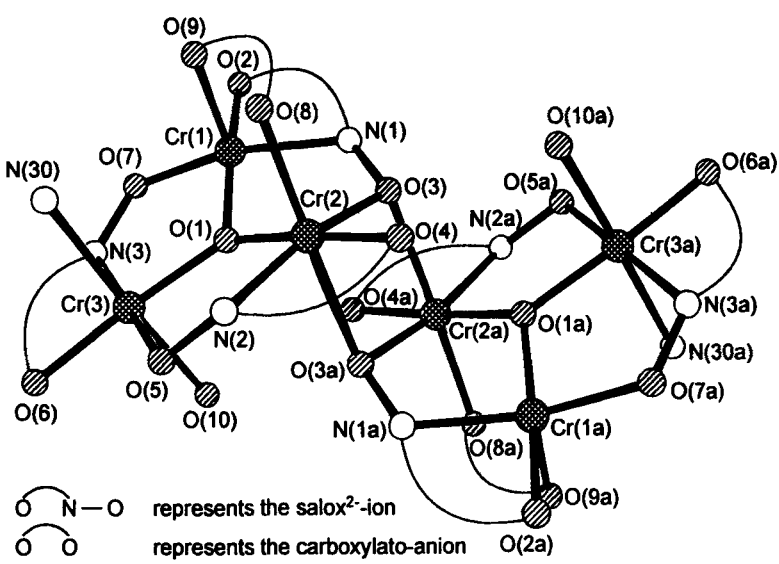

Figure 9. Structure of the Cr(III) coordination spheres in the hexanuclear complex.

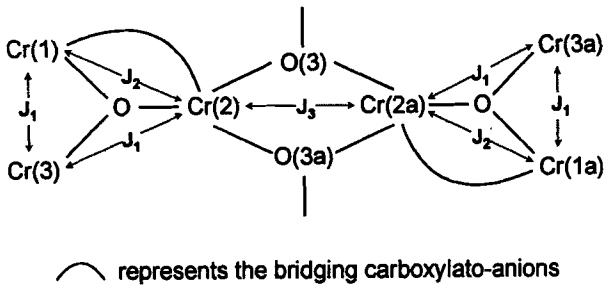

Chart 3. Coupling model.

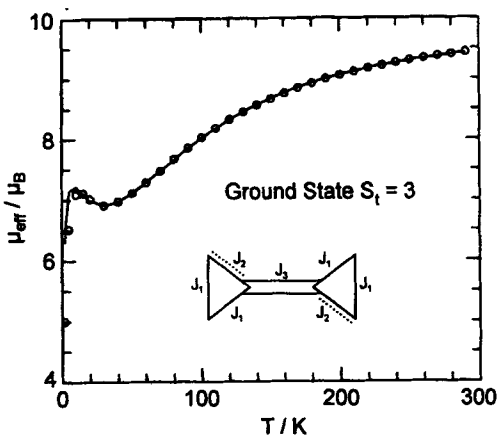

Figure 10. A plot of μ_{eff} vs T for the $[Cr(III)]_6$-complex. The solid line is the calculated curve using irreducible tensor operators.

$Cr(2)NO_5$ and $Cr(3)N_2O_4$ coordination spheres, whereas Cr(1) is in an unusual *square-pyramidal* $Cr(1)NO_4$ environment. The Cr(1) centre provides another of the very few examples of an authenticated non-octahedral Cr^{III} complex.

The exchange coupling model (chart 3) was considered for simulation of the experimental magnetic data using the irreducible tensor operator (ITO)[26] mathematical method with the Heisenberg Hamiltonian in the form $H = -2JS_i \cdot S_j$.

The best fit, shown as the solid line in figure 10, yields the following parameters:

$$J_1 = -14{\cdot}2\ cm^{-1},\ J_2 = +12{\cdot}8\ cm^{-1},\ J_3 = +5{\cdot}3\ cm^{-1},\ g = 2{\cdot}13.$$

The ground state $S_t = 3$, lying $18{\cdot}4\ cm^{-1}$ below the first excited state $S_t = 2$, is also confirmed by the field-dependent magnetization study at 5 K in the 0·5–6·5 T magnetic field range; a value of $3{\cdot}03\ cm^{-1}$ is obtained for the zero-field splitting parameter D.

4. Concluding remarks

We have tried to narrow the gap prevailing so long in the area of coordination chemistry of salicylaldoxime with trivalent transition metal ions. Of particular interest is the

dramatic effect of bridging ligands like carboxylato anions for cooperation with the ancillary ligand, viz. salicylaldoxime, to build-up high-nuclearity metal clusters. This phenomenon is not confined to salicylaldoxime alone, and in fact, fascinating chemistry is emerging with other phenol-containing oximes.

Electrochemical methods together with magnetic measurements have been proved to be very useful tools to generate phenoxyl radical species, not only in solution but also as crystalline materials; work is in progress to study the interactions of radicals with transition metal ions in polynuclear complexes.

Although most of the compounds have been structurally characterized, little can be said about magneto-structural trends. In the light of our findings on the tetranuclear complexes with different bridging carboxylate ligands, it is clear that a small perturbation arising from the apparently "innocent R" groups of the carboxylic acids that does not involve a direct interaction with the magnetic orbitals, can lead to ground state-variability. This observation is potentially relevant for the determination of the electronic structures of the metalloproteins.

A problem concerning the exchange coupled systems is the unavailability of isostructural polynuclear complexes with varying d^n electron configurations. It remains to be seen whether such isostructural systems, now available for salicylaldoxime, can be extended to other derivatives of salicylaldoxime.

The oxime moiety ($-C(R) = NO^-$) combined with a coordination site for a metal ion, represents a bridge between coordination complexes and supramolecular assembly. We will explore the possibility in future studies.

Acknowledgements

Financial support from the Fonds der Chemischen Industrie is acknowledged. I wish to thank warmly my coworkers and colleagues involved in this work, and Prof K Wieghardt for his continuous support.

References

1. Ephraim F 1930 *Berichte* **63** 1928
2. Cox E G, Pinkard F W, Wardlaw W and Webster K C 1935 *J. Chem. Soc.* 459
3. Jarski M A and Lingafelter E C 1964 *Acta Crystallogr.* **17** 1109
4. Srivastava R C, Lingafelter E C and Jain P C 1967 *Acta Crystallogr.* **22** 922
5. Orioli P L, Lingafelter E C and Brown B W 1964 *Acta Crystallogr.* **17** 1113
6. Merritt L L, Gaure C and Lessor A E 1956 *Acta Crystallogr.* **9** 253
7. Pfluger C E and Harlow R L 1970 *Acta Crystallogr.* **B26** 1631
8. Grigg J, Collison D, Garner C D, Helliwell M, Tasker P A and Thorpe J M 1993 *J. Chem. Soc., Chem. Commun.* 1807
9. Bielig H-J and Möllinger H 1957 *Liebigs Ann. Chem.* **605** 117
10. Toyota E, Umakoshi K and Yamamoto Y 1995 *Bull. Chem. Soc. Jpn.* **68** 858
11. Liu S, Zhu H and Jubieta J 1989 *Polyhedron* **8** 2473
12. Zerbib V, Robert F and Gouzerh P 1994 *J. Chem. Soc., Chem. Commun.* 2179
13. Potocnak I, Heinemann F W, Rausch M and Steinborn D 1997 *Acta Crystallogr.* **C53** 54
14. Rettig S J, Storr A and Trotter J 1992 *Acta Crystallogr.* **C48** 1587
15. Manolov K R 1967 *Russ. J. Inorg. Chem.* **12** 1431
16. Chaudhuri P, Flörke U and Winter M (unpublished results)
17. Bill E, Krebs C, Winter M, Gerdan M, Trautwein A X, Flörke U, Haupt H-J and Chaudhuri P 1997 *Chem. Eur. J.* **3** 193
18. Chaudhuri P, Hess M, Weyhermüller T, Bill E, Haupt H-J and Flörke U 1998 *Inorg. Chem. Commun.* **1** 39

19. Taylor S W, Cashion J D, Brown L J, Hawkins C J and Hanson G R 1995 *Inorg. Chem.* **34** 1487, and references therein
20. Olah G A, Arvanaghi M and Surya Prakash G K 1980 *Synthesis* 220
21. Hendrickson D N 1993 In *Research frontiers in magnetochemistry* (ed.) C J O'Connor (World Scientific: Singapore) p. 87
22. Kahn O 1997 *Chem. Phys. Lett.* **265** 109
23. Chaudhuri P, Winter M, Fleischhauer P, Haase W, Flörke U and Haupt H-J 1993 *J. Chem. Soc., Chem. Commun.* 566
24. Chaudhuri P, Birkelbach F, Winter M, Staemmler V, Fleischhauer P, Haase W, Flörke U and Haupt H-J 1994 *J. Chem. Soc., Dalton Trans.* 2313
25. Chaudhuri P, Hess M, Rentschler E, Weyhermüller T and Flörke U 1998 *New J. Chem.* 553
26. Gatteschi D and Pardi L 1993 *Gazz. Chim. Ital.* **123** 231